Electronic Theses and Dissertations

2022

Design of Affordable Polyaniline - Based Wearable Sensor for Real Time Plant Growth Monitoring

Temitope Borode

South Dakota State University, temitope.borode@yahoo.com

DESIGN OF AFFORDABLE POLYANILINE - BASED WEARABLE SENSOR FOR

REAL TIME PLANT GROWTH MONITORING

BY

TEMITOPE BORODE

A thesis submitted in partial fulfillment of the requirements for the

Master of Science

Major in Mechanical Engineering

South Dakota State University

2022

THESIS ACCEPTANCE PAGE

Temitope Borode

This thesis is approved as a creditable and independent investigation by a candidate for the master's degree and is acceptable for meeting the thesis requirements for this degree. Acceptance of this does not imply that the conclusions reached by the candidate are necessarily the conclusions of the major department.

Anamika Prasad
Advisor   Date

Yucheng Liu
Department Head   Date

Nicole Lounsbery, PhD
Director, Graduate School   Date

ACKNOWLEDGEMENTS

My profound gratitude to God Almighty for His infinite mercy during my study in South Dakota State University. My appreciation goes to my advisor Dr. Anamika Prasad, for her guidance, advice, and effort towards the completion of this work.

I would like to thank my graduate committee members: Dr. Todd Letcher, Dr. Zhong Hu, and Dr. Crystal Levesque for their support and advice toward the completion of my program. My appreciation goes to Dr. Yucheng Liu for offering me a graduate assistantship position in my concluding semester.

Finally, I would like to appreciate my wife, my parents and sibling for their support during my time in South Dakota

TABLE OF CONTENTS

ABBREVIATIONS

ANI   Aniline

APS   Ammonium persulfate

Au   Gold

CNT   Carbon nanotubes

DMM   Digital multimeter

HCl   Hydrochloric acid

PDMS   Polydimethylsiloxane

Ti   Titanium

mm   Millimeters

μm   Micrometers

ΔR Change in resistance

R_o Initial resistance

RGR   Relative growth rate

LA   Leaf area

LIST OF FIGURES

LIST OF TABLES

ABSTRACT

DESIGN OF AFFORDABLE POLYANILINE - BASED WEARABLE SENSOR FOR

REAL TIME PLANT GROWTH MONITORING

Temitope Borode

2022

The need for precision agriculture in today and future farming cannot be overstressed. Recent agriculture is characterized by numerous challenges such as environmental stressors and resource constraints resulting in low crop yield and unsustainable agriculture practices. Understanding plant growth mechanism and growth rate under the external influence is a bedrock towards precision agriculture practices ensuring optimum yield and sustainable utilization of resources. The current study addresses this need by developing and applying an affordable and stable sensor for monitoring plant growth. The sensor was fabricated by *in-situ* chemical polymerization of aniline on an elastic band substrate by dip coating. The sensor was characterized using optical imaging and Fourier-transformed infrared spectroscopy (FTIR), calibrated for strain sensing, and its stability was analyzed under cycling loading and temperature variations. When applied to sunflower and soybean stems, the sensor detected a rhythmic growth pattern with higher growth during the dark cycle in sunflower plants but a continuous growth for both the light and dark cycle for soybean. The similarities between growth rate and growth pattern observed on these plants with available information on plant growth indicate the fitness of the sensor for

such precision measurement for plant health and suggest a step towards the development of precision sensing capability for agriculture.

CHAPTER 1

INTRODUCTION

Plants provide the fundamental basics for all life on the earth [1]. Its importance to life ranges beyond providing provision of food. Plants are key for regulation of ecosystem functions (flood, erosion, as carbon monoxide sink) [2], function as sources of natural fibers for renewable industries [3]–[5] , disease prevention [6] and other extensive use in drug industries among others.[7] However, plant are also under increasing threat from multiple directions [1]. Food shortage due to rapid growing world population [8], soil and water contamination resulting from excessive use of fertilizer [9], and water wastages from irrigation [10] has put new demands on plant and agriculture practices. Monitoring and measuring plant growth under environmental influence and other stressors provides an avenue for better understanding of plant health as a function of resource utilization. Hence the need for smart farming to harvest information about plant growth is instrumental towards ensuring optimum yield and sustainable utilization of resources.

Existing method for measuring plant growth and health such as imaging and image processing, hyperspectral imaging, satellite imaging, and infrared sensors has been reported to provide information about plant growth, stress, and growth level [11]–[14]. Raman Spectroscopy has also been used to capture molecular composition of plant stem under healthy and nutritional stressed condition [15]. However, while these methods have high utilization, they require expensive gadgets to set up, special skills to operate, and may lag in time before the knowledge is actionable in the farm. Hence, the need for smart farming and optimization of resource utilization demands affordable real-time plant

health measurement capability such as plant growth monitoring using strain-sensing or disease monitoring via chemical sensing.

Recent development and deployment of smart sensor in agriculture has attracted a lot of attention. Examples include plant sensors for plant health monitoring under drought, soil saline and biotic stresses [16]–[19]. In another work, a strain sensor using carbon nanotube (CNT)/graphite and chitosan/graphite ink was developed and attached to a fruit to measure its change in diameter with growth [20], [21]. While these measurements were effective of tracking fruit growth, in plant life cycle, fruit growth appear later in life (reproductive stage) while the early growth stages (vegetative stage) show greater sensitivity and demand for resources [22]. In another study, multiple sensor and sensing platform were developed for plant health and microclimate monitoring [23]. It included a leaf growth sensing made from gold pattern deposited on pre-stretched polydimethylsiloxane (PDMS). The Au/PDMS strain sensor showed high sensitivity to micro-growth on leaf for micro-scale investigation. These studies together highlight recent developments in agriculture sensing. To take the field forward, there is a need to monitor plant growth during the early stages of growth and connecting growth to fertilizer and water usage to not only monitor plant health, but also optimize water and fertilizer usage. At the same time, there is a need for affordability in sensing design to make it effective for its large-scale utilization from large and small farms to hobbyist farmers.

Herein, we report the development and application of a polyaniline (PANI) based strain sensor for monitoring plant growth. Polyaniline, the most studied one - dimensional conductive polymer with reported properties like large surface area, large conductivity,

porosity, ease of synthesis and fast diffusion of gas molecules has attracted attention in gas and chemical sensing [24]–[28]. PANI-based composite for strain sensing has also been recently reported [29]–[31]. Here we develop PANI based sensor through *in-situ* chemical polymerization of aniline applied to common elastic band and use the sensor for sunflower and soybean plant growth monitoring at their early stages of growth. The paper presents a comprehensive work from sensor development, plant growth experiments, and application and outcome of the sensor for real-time growth monitoring.

CHAPTER 2

LITERATURE REVIEW

2.1 Role of Plants in the Ecosystem

The role of plants in the ecosystem is crucial, plant are one of the two important living organisms, they contributed immensely to the function of the biosphere. Unlike animal, plants can manufacture their food by harvesting energy from sunlight and utilizing for nutrient manufacturing through photosynthesis. Other organisms depend on excess food manufactured by plants for survival. Plant do not only make food for other organisms, but they also serve as source of shelter, clothing, and medicine for other organism in the ecosystem. The role of plant in the ecosystem extends beyond food shelter and clothing, plants also play major role in climate regulation by releasing oxygen to enrich the air, which is breathed in by animals and recycling the CO_2 released by other organisms [32].

2.2 Plant Growth and Development

Plants shows open form of growth, plants growth which is the increase in length and grith are unlimited during their life cycle. In contrast animal growth are limited at adult stage, except for certain organisms who experience organ regeneration.

Meristems are responsible for plant unlimited growth; meristems are stem cells which multiplies through cell division in plants. The formation of fresh tissue and organs in plant is due to meristematic activities resulting in increase in height and grith, this type of growth in plant is termed open growth. The growth in plant stem maybe classified into two types, namely primary growth, and secondary growth. Primary growth occurs at the apical meristem of plant, this is the tip of the shoot(stem) and root, called shoot apical. The internode below the apical meristem is also a site for plant longitudinal growth, in

certain plants other internodes stop growing as the plant ages. Secondary growth on the other hand is the stem grith increase which occur due to the activities of lateral meristem at the side of a shoot or root [22]. Plants are expose to certain harsh conditions during their life cycle, which negatively impact their growth or may lead to death. These harsh conditions are termed plant stresses.

2.3 Introduction to Plant Stresses

In 1822 stress was introduce to the theory of elasticity. In physic stress can be defined as force per unit area, is a measure of the intensity of the total internal forces acting within a body across imaginary internal surfaces, as a reaction to external applied forces and body forces [33]. In another study, stress was define as a quantity that describes the magnitude of forces that cause deformation [34]. This definition simply means stress when applied on a material, causes deformation of the material, which can be reversible or permanent based on the material properties, time of application and magnitude. Just like in physics and engineering definitions has been formulated for plant stresses. In a study, Plant stress was defined as any unfavorable condition or substances that affect or block a plant's metabolism and development [35]. In another study, stress was defined as "changes in physiology that occur when species are exposed to unfavorable conditions that need not represent a threat to life but will induce an alarm response"[36]. The most study plant stress is environmental stress, the two type of environmental stress are namely, biotic stresses and abiotic stresses.

Abiotic stresses are stresses imposed on plants from environmental factors, such as temperature, drought (water stresses), excessive watering, soil salinity, soil toxicity, wound and nutrition negatively impact plants growth or development resulting into low

crop yield. Biotic stresses on the other hand are stress imposed on plant through interaction with other organisms, such as pathogens, bacterial, fungi, pest among others. Plant naturally develop defense against stress through resistance genes and emission of volatile organic compounds, however excessive stress exposure may lead to plants death. [37], [38]

2.4 Plant Growth Measurement

Plant growth monitoring is crucial in agricultural practices, monitoring and measuring plant growth provides information towards achieving optimum crop yield, optimum utilization of resources and as well provides knowledge on the interaction of plant with their environment. The conventional method for plant growth monitoring is RGR, LA, imaging, and image analysis [39]. However, RGR and LA are inversive approach of growth measurement while Imaging requires expensive gadget and high skills to operate. Strain sensors has been recently developed by researchers for real time non inversive plant growth monitoring.

2.5 Strain sensors

Strain sensors (gauges) are devices that varies in electrical resistance because of changes in strain (increasing or decreasing dimension). The electrical properties of strain gauges vary due to applied force which changes the dimension. Strain is the displacement or deformation of a material due to an applied stress. On the other hand, stress is the force applied to a material divided by its cross sectional area [40]. Strain gauges such as linear strain gauges, strain gauge rosettes, membrane rosette strain gauges and rectangular strain gauges has been used in engineering applications, aircraft, railroad, and other industries for displacement measurement [41]. Recently film strain sensor made for

conducting layer such as carbon nanotubes, graphene, metal oxides, graphite, gold and conducting polymer has been used for strain measurement by researchers. Conducting polymer such as polyacetylene (PA), polyaniline (PANI), polypyrrole (PPy), polythiophene (PTH), poly(para-phenylene) (PPP), poly(phenylenevinylene) (PPV), and polyfuran (PF) synthesized through simple chemical polymerization, is current used in fabrication of strain sensor because of their easy of synthesis, low cost and excellent electrical properties [42], [43].

CHAPTER 3

METHODOLOGY

3.1 Material and Method

3.1.2 Materials

All chemicals for sensor development were purchased from Sigma Aldrich ACS reagent grade and included Hydrochloric acid HCl (37 wt.%), Aniline (C6H7N), and Ammonium Persulfate or APS (NH4)2S2O8. Common market available elastic band and polyethylene resin sheet was purchased for use as sensor substrate and sensor attachment to the plant, respectively.

3.1.3 Synthesis of Polyaniline and Sensor Fabrication

Figure 1 shows PANI synthesis and the sensor fabrication process. Specifically, the PANI nanoparticles was synthesized by chemical oxidative polymerization of aniline in HCl following protocol described earlier [44], [45]. To do so, 4 ml of aniline (99.5 wt.%) was dissolved in 50 ml 1M HCl under constant stirring with a magnetic bar at 250 rpm until a clear solution of HCl/Aniline was obtained (Figure 1a). The HCl/Aniline solution was place in ice bath to lower the temperature below 0^0C. Separately, a solution for APS was also prepared by dissolving 5 grams of APS in 50 ml distilled water (Figure 1b). Next, two approaches were taken to (a) synthesis only PANI for material characterization, and (b) synthesis PANI nanoparticles in presence of the elastic band (PANI/Elastic band) through *in-situ* dip coating for sensor application. For PANI only synthesis, the APS solution was drop wise added to the HCl/aniline ice bath solution for 1 hour under constant stirring at 250 rpm. The solution was made to sit for 1hour after, then vacuum

filtered and washed with 1M HCl and distill water to obtain a dark green precipitated clay. The obtained clay was dried at 60^0 C in the oven overnight to get PANI (Figure 1c).

For PANI/elastic band sensor synthesis, the process involved *in-situ* dip coating of PANI nanoparticles on the elastic band during polymerization process [46]. The PANI synthesis steps were same as described earlier. However elastic band (width 3.1 mm, length 20 mm) was added to the solution of HCl/aniline before polymerization as marked in Figure 1d. The solution was placed in ice bath and the APS solution was drop wise added as before. The solution was made to sit for 1hour to allow complete polymerization and full coating of PANI nanoparticles on the elastic band fiber, after which the obtained green elastic band was washed with 1M HCl and distill water and oven-dried at 25^0C overnight. Figure 2 shows the fabricated PANI/elastic band strain sensor. In Figure 2a, the sensor is shown wrapped with a polyethylene resin sheet to avoid moisture during measurement, while Figure 2b depict the sensor in folded form indicating its flexibility.
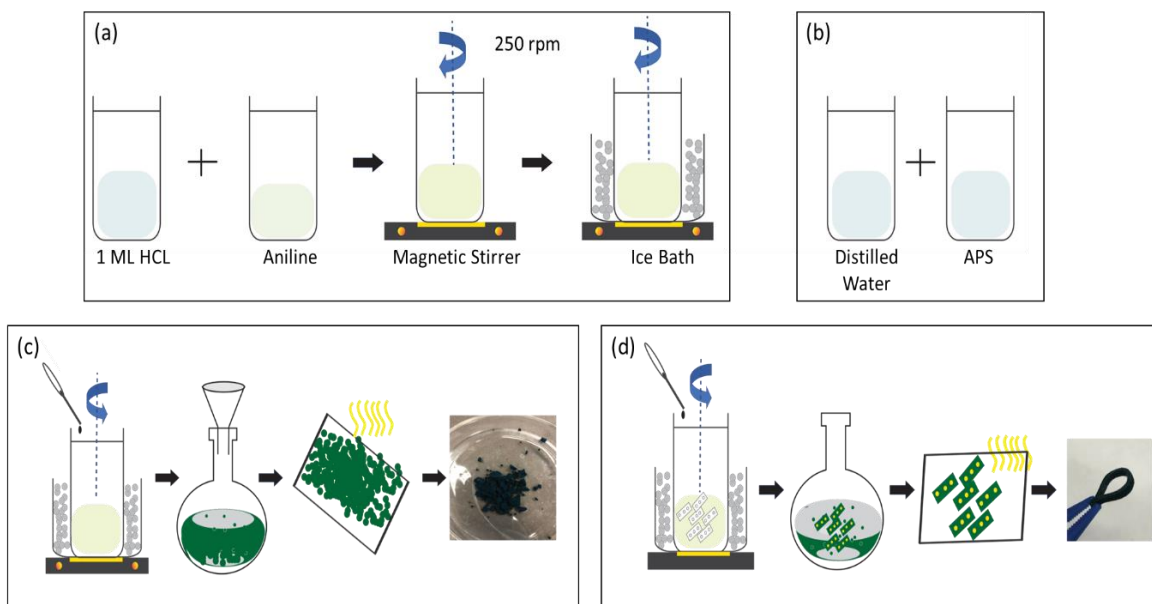
Figure 1: *PANI synthesis and sensor fabrication process. (a) Preparation of Hydrochloric acid (HCl)/Aniline solution through mixing under constant stirring and colling to 0^0C in an ice bath (b) Preparation of ammonium persulfate (APS) solution in distilled water, and (c) Chemical polymerization of PANI by drop wise addition of APS to HCl/Aniline solution under constant stirring at 0^0C (c) Sensor fabrication via in situ dip coating of elastic band during chemical polymerization of PANI nanoparticles.*

3.1.4 Sensor Characterization

Fourier transformed infrared spectroscopy (FTIR) study was performed using Perkin Elmer Spectrum 65 FTIR Spectrometer to characterize the PANI clay composition. Digital optical microscopy VHX-600 (Keyence, USA) was performed on the elastic band before and after polymerization to understand the morphology of PANI/elastic band strain sensor.

3.1.5 Sensor Calibration

Figure 3 shows the inhouse tensile system set up used to investigate the performance of the sensor. The setup included a vernier caliper held in position with a clamp and tripod stand (stand partially visible in the figure). The sensor was mounted on the vernier jaw using a two-sided release tape (Figure 3a). The movable jaw was manually shifted in the arrow direction shown in the figure using the thumb grip slider of the vernier caliper to apply tensile strain (Figure 3a). Each rotation of the thumb grip exerted an average of 0.45 mm tensile stretch on the sensor, with the elongation monitored through the calibrated digital display of the Vernier caliper and converted to strain using the expression $\Delta l/l_0$, where Δl and l_0 are the change in length and initial length respectively. The change in relative resistance of the sensor in response to strain was measure by two-probe system using Keysight 34460A digital multimeter. The two-sided release tape insulated the resistance reading from the metallic vernier frame.

The initial length of the sensor (l_0) was 15.5 mm as indicated in the figure. A total uniaxial tensile stretch of 100% was applied with roughly equal 10% step increase, controlled through rotation of the thumb screw. Additionally, multiple repeats of the loading and unloading (indicated by the double-headed arrow of Figure 3b) were done to evaluate sensor stability. A stopper was used to keep the slider load/unload within the region of measurement interest.

The sensor stability for long time measurements was also explored. To do so, the sensor was kept in a covered glass bottle for five days at room temperature and its resistance measured each day. Finally, temperature sensitivity of the sensor was also investigated. To do so, the sensor was place it in a programmable temperature oven, the oven

temperature raised from 20^0 C to 100^0 C with 10^0 C step increase. The change in relative resistance was recorded by connecting the sensor inside the oven to the digital multimeter placed outside using a low resistance wire.
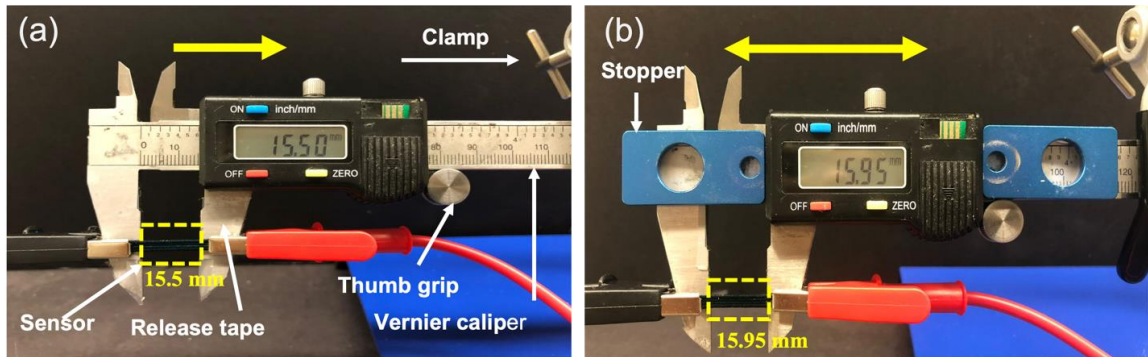
Figure 2: *The strain sensor tensile test system, showing (a) tensile stretch setup with the sensor (15.5mm) held between the vernier caliper jaws and the arrow showing stretch direction, (b) respeated load/unload test system setup with the double-sided arrow showing the direction of loading and unloading, and a stopper used to maintain within the region of measurement interest.*

3.1.6 Plant Growth Experiment setup

Real-time plant growth rate measurement was performed on sunflower and soybean, which are plants of economic importance. Sunflower was grown in greenhouse environment while soybean was grown in a growth chamber located in the University's shared facility. Both plants were exposed to 16 hours light cycle and 8 hours dark cycle. Once the plants were ready for measurement, they were transferred to a growth rack in the lab for measurement to avoid logistical issues such as noise from motion of other users in the shared facility and leaving the data logger overnight for measurement. indoor lab was maintained at a room temperature of approximately 21 ^{0}C and the humidity at

25% using a humidifier, these values logged using standard temperature and humidity logger. The plants were left in the indoor growth tent for 1 week before measurement to allow them to acclimatize to the growth condition.

Figure 4 depicts the sensor integration on sunflower (Figure 4a and 4b) and soybean (Figure 4c and 4d). To measure the plant growth rate, the sensor was mounted on the internode below the apical meristem (shown by solid lines in the figure) of sunflower and soybean 2 weeks and 3 weeks after planting respectively. The time gap between planting and growth rate measurement was set to allow reasonable stem strength needed for sensor anchorage. A two-sided release tape was used to attach the ends of the sensor to the plant. The sensor attachment follows similar protocol in earlier studies [20], [21]. The sensor was connected to a data acquisition device (Keysight 34460A) using a low resistance copper wire and data logged using Keysight BenchVue software. The copper wire connector was immobilized on the rack to avoid deflection during measurement. The sensor was 20 mm long, 3.1 mm width and 0.3 mm thick, with ends fixed and flexible central part of 15.50 mm used in the measurement. Sunflower growth was monitored for two consecutive days, measurement was taken for 24 hours stating from 5 pm. Day 2 measurement was taken few minutes after day 1 measurement without disturbing or adjusting the sensor. Soybean growth was also monitored and measured over 24 hours starting from 6.52 pm.
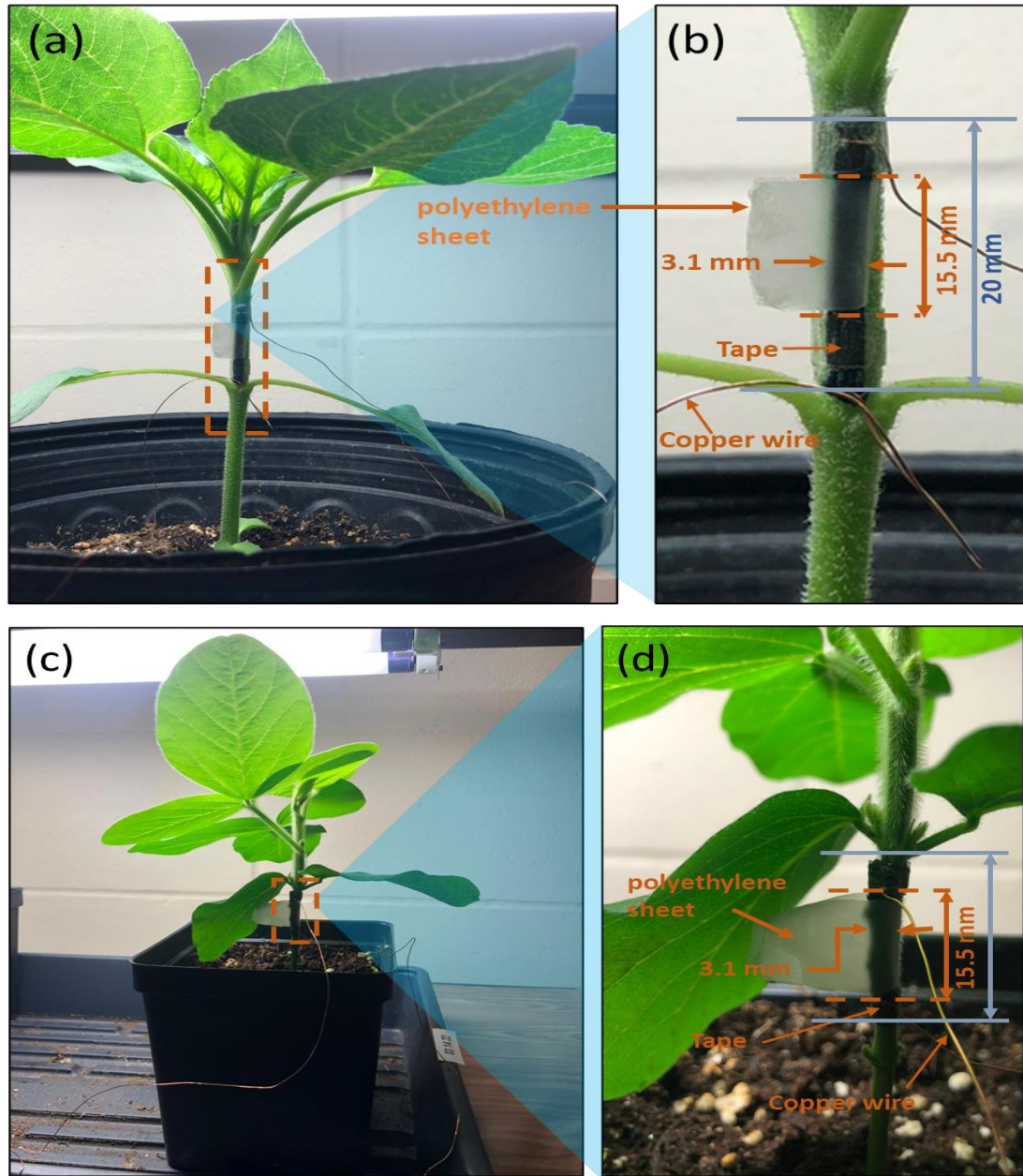
Figure 3: Real-time plant growth monitoring with the strain sensor mounted on sunflower(a and b) and soybean (c and d). In each case, the sensor was attached to the plant using a two-sided tape, The band total length was 20 mm long, 3.1 mm width and 0.3 mm thick with the end fixed to the plant stem with two sided adhesive tape. The stretchable part of the sensor from which resistance was measured was 15.5 mm. The sensor was wrapped in polyethylene sheet to avoid moisture contact.

CHAPTER 4

RESULTS AND DISCUSSION

4.1 Result

Figure 4 shows the fabricated PANI/elastic band strain sensor. In Figure 4a, the sensor is wrapped with a polyethylene resin sheet to avoid moisture during measurement, while Figure 4b depicts the sensor in folded form, indicating its flexibility. The section below discusses the outcome of the sensor characterization, sensor calibration, and its use for real-time plant growth measurement.
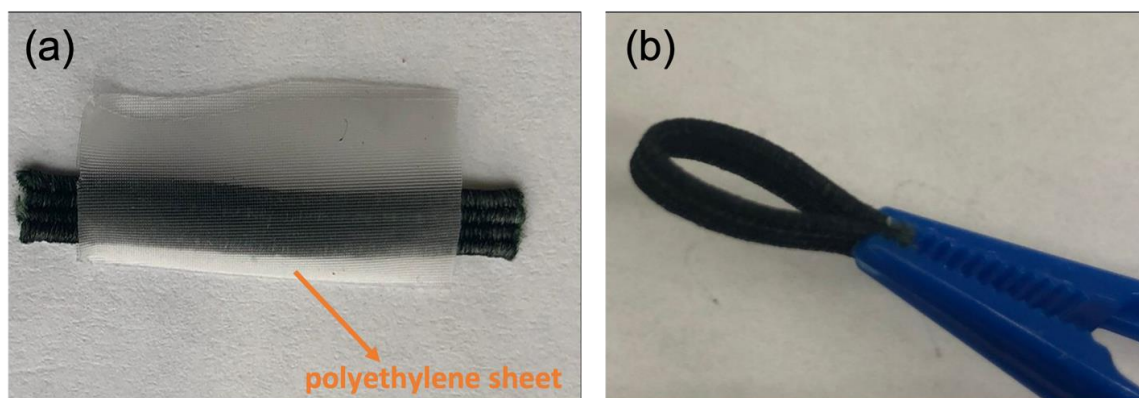
Figure 4: Image of synthesized PANI/elastic band strain sensor (a) PANI/elastic band strain sensor wrapped in a polyethylene sheet. (b) PANI/elastic band strain sensor in folded form indicating flexibility.

4.1.1 Sensor Characterization

The morphology of the sensor was investigated using optical electron microscopy (Keyence, USA). Figure 5a to c shows the elastic band before coating, with Figures 5b and c showing its glossy white fiber strand. The arrow in these figures indicates the gaps between the fiber strands. Figures 5d to f shows the fiber post dip coating with PANI, which indicates changed structure as a result. The fibers now appeared as rough bright

deep green with PANI nanoparticles filling the gaps between the fibers indicated by the arrow. The PANI nanoparticles bonded to the elastic fibers giving a roughened appearance to their surface.

Figure 6 shows the FTIR spectra of the HCl doped PANI clay, with peaks assigned based on literature and listed in Table 1. The absorption peak 1558 cm^{-1} and 1475 cm^{-1} are assigned to C=C stretching of quinonoid and benzenoid ring, respectively. The two peak 1287 cm^{-1} and 1237 cm^{-1} are assigned to C-N stretching of secondary aromatic amine, and BBB. The peak 876 cm^{-1} is attributed to C-H out of plane bending vibration of two adjacent hydrogen atom in a 1, 4 - distributed benzene ring. The obtained peaks closely agree with PANI spectra peaks previously reported [47]–[50]. Hence, the prepared PANI clay was doped.
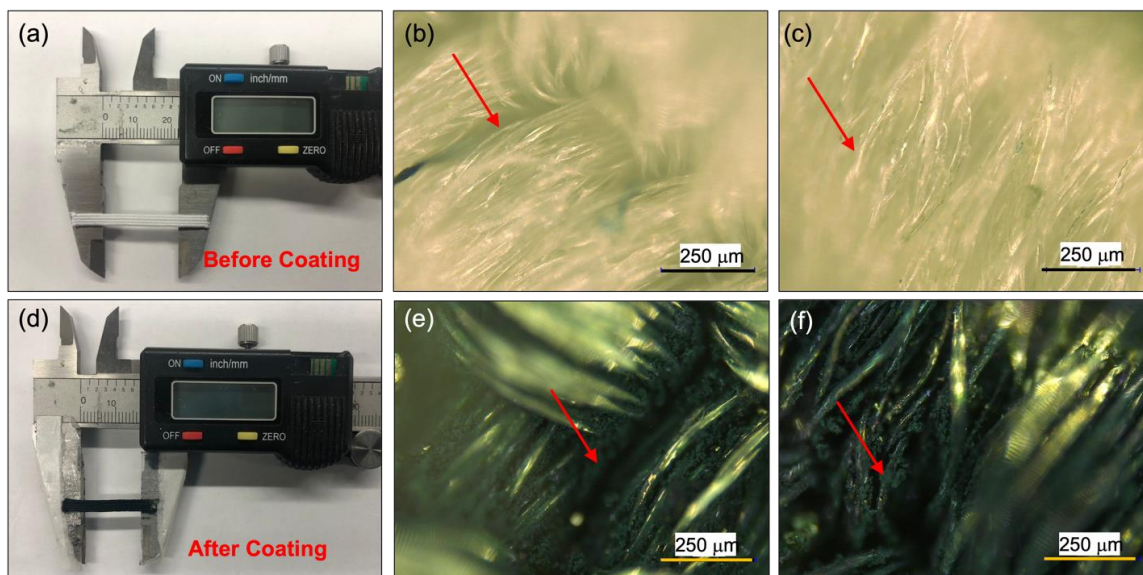
Figure 5: *Strain sensor showing (a) elastic band before polymerization, (b and c) optical microscopy image of as-is band showing a knitted white fiber, (d) green-colored elastic band after polymerization, and (e and f) optical microscopy image showing PANI nanoparticles filling the gaps between the fibers.*
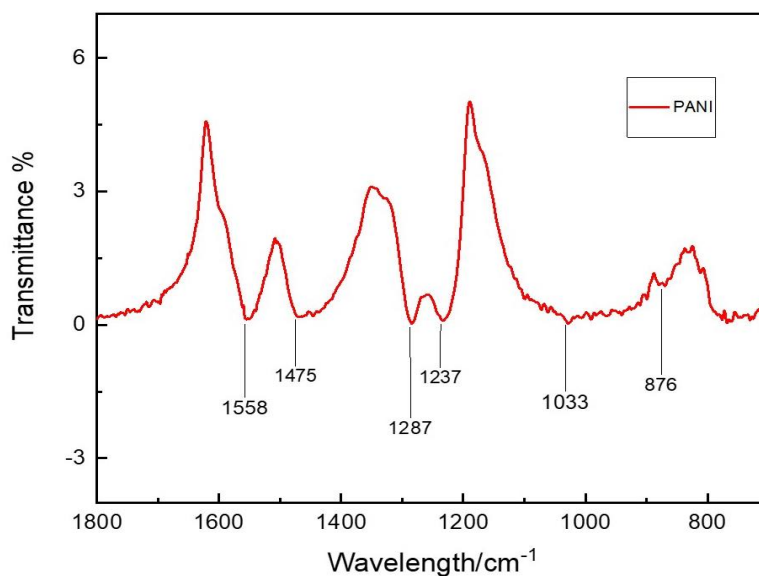
Figure 6: *FTIR signature of PANI clay showing assigned peak attributed to HCl doped Polyaniline. The peaks were assigned based on previous studies in the table below*

Table 1: *Assignments of the FTIR wavelengths for synthesized PANI*

Wavelength (cm-1)	Assignment	References
1558	Quinonoid (Q) ring stretching	[47], [49]–[51]
1475	Benzenoid (B) ring stretching	[47], [49]–[51]
1287	C-N stretching of secondary aromatic amine	[47], [49]–[51]
1237	C-N stretching in BBB unit	[47], [49]–[51]
1033	HSO^{4-}/SO^{3-} group on sulfonated aromatic ring	[47], [49]–[51]
876	C-H out-of-plane deformation for 1,4-disubstituted ring	[47], [49]–[51]

4.1.2 Sensor Calibration and Outcome

The elastic band strain sensor responded to 100% applied strain with 10% step increase corresponding to 1.55mm step stretch and 15.5mm total stretch. The relative resistance was obtained using the expression $\frac{\Delta R}{R_0}$, where ΔR and R_0 are the change in resistance and initial resistance respectively. Figure 7a depicts how the sensor relative resistance increases in response to increasing strain loading, the $\frac{\Delta R}{R_0}$ increases as the sensor increase in length when stretched. The gauge factor (GF) which is the sensor strain sensitivity was 3.8 at 10% strain and 2.5 over 50% strain region, this was obtained by using the expression $\left(\frac{\Delta R}{R_0}/\varepsilon\right)$, where ε is the strain. The sensor was subjected to cycle strain loading (stretch and release), 0.45mm tensile stretch was applied on the sensor repeatedly 100 times as depleted in Figure 7b. The sensor $\frac{\Delta R}{R_0}$ increases in response multiple loading returns to the initial value after each unloading. The sensor was also sensitive to temperature, Figure 7c shows a step increase in relative resistance due to increasing temperature, however a stable relative resistance was observed between 20^0C and 30^0C. The sensor shows good stability in successive five days, as only slight non-significant resistance change was observed (Figure 7d).
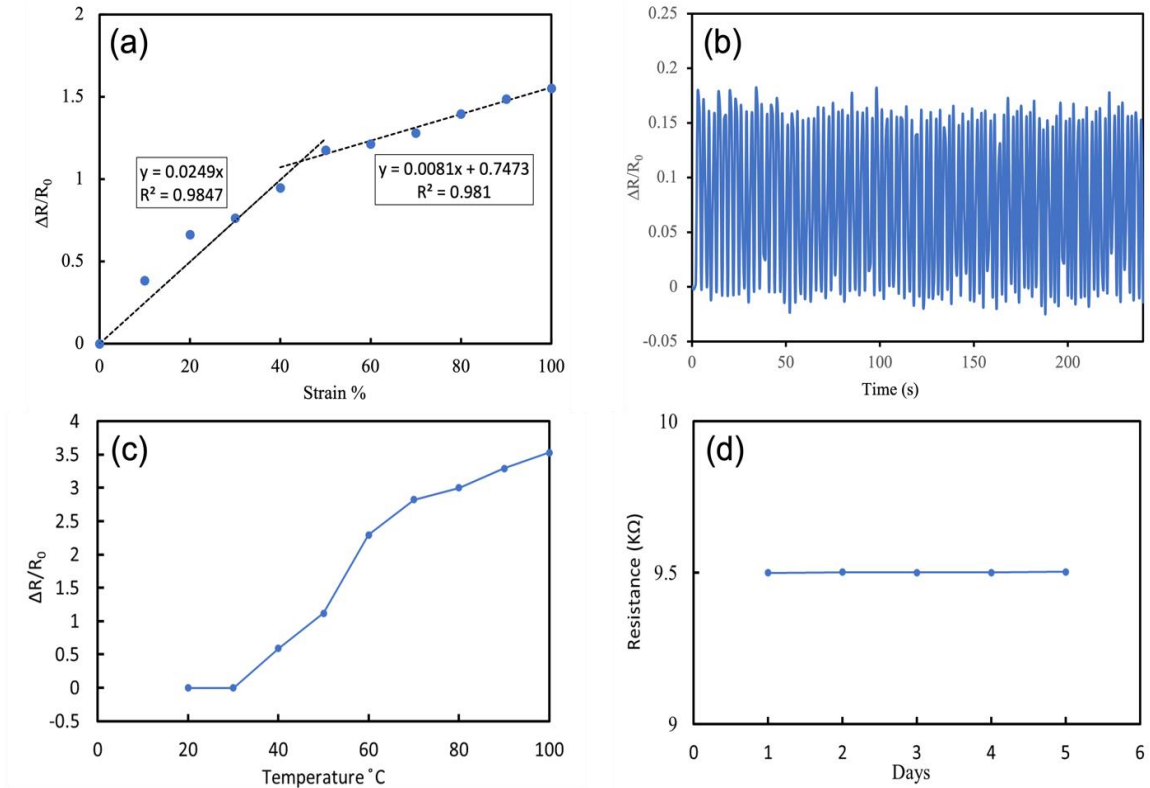
Figure 7: *The strain sensor performance under test. (a) A plot of relative resistance and strain, showing the gradual increase in resistance in response increasing tensile strain. (b) A plot of relative resistance and time, showing sensor stability under 100 cycle 0.45mm repeated Tensile loading and unloading (c) A plot of relative resistance and temperature, showing increasing relative resistance in respose to temperature variation, with a stable resistance observed up to 300C. (d) A plot of resistance and time, showing sensor stability in five days, no significant resistance change was obsered*

4.1.3 Realtime plant growths measurement

Figure 8 shows the outcome when the sensor was applied for real-time growth pattern measurement on sunflower over 2 days. The measurement was started in the evening around 5 pm, which corresponds to time 0 on the graph. Day2 reading immediately followed day1 after sensor readjustment to set back to its unstrained stage as mentioned earlier.

 Day1 curve shows the following pattern via changes in relative resistance ($\Delta R/R_0$) (a) a low gradient in the first five hours, among them the first three hours were in the light

cycle, (b) the gradient linearly increases for the next nine hours, first six of which were in the dark cycle, and (c) the resistance becomes stable for the next six hours of light cycle, and then begins to increase again. Day 2 curve follows similar pattern as day 1, though shows a more rapid increase in the last three hours of measurement in the light cycle. A total $\Delta R/R_0$ amassed by our strain sensor includes 0.43 day 1 and 0.57 day 2. From the sensor calibration curve, the relative resistance change corresponds to 17.3% strain or 267 mm increase day 1 and 22.9% strain or 355 mm increase day 2, to a total increase of 622 mm over the 2 days monitored, indicating a rapid growth period.

Figure 9 shows the growth pattern observed in soybean plant. Soybean plant experienced a linear gradient increase throughout, both in dark cycle (8 hours) and light cycle (16 hours) periods. A total $\Delta R/R_0$ amassed by our strain sensor in 24 hour was 0.6, corresponding to approximately 373 mm stretch.
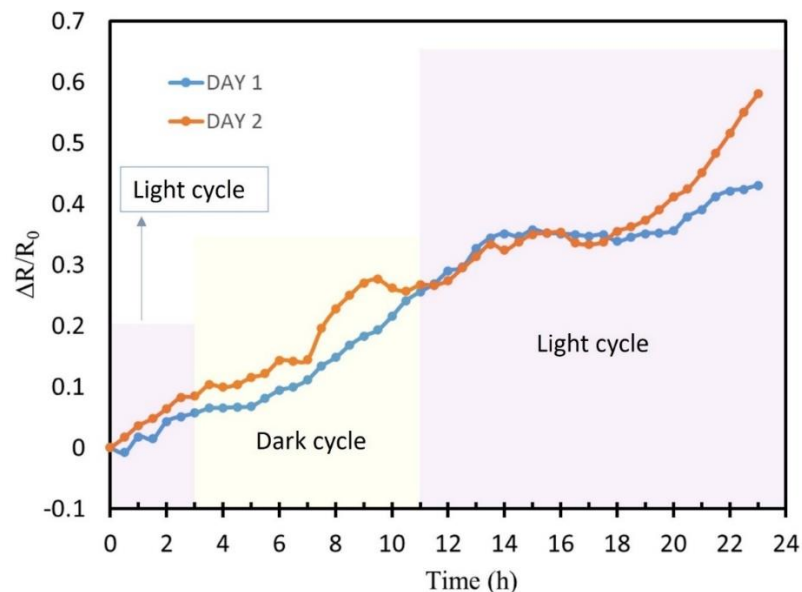
Figure 8: Realtime Plant growth measurement. Image showing a patterned stepwise increase in sunflower growth over 24 hours in two consecutive days,rapid growth growth was observed during dark cycle while the light cycle was characterised with near stable

growth. total ΔR/R$_0$ amassed in day 1(24 hours) was 0.43 and on day2 of 0.53, corresponding to approximately 622μm growth in 2 day .
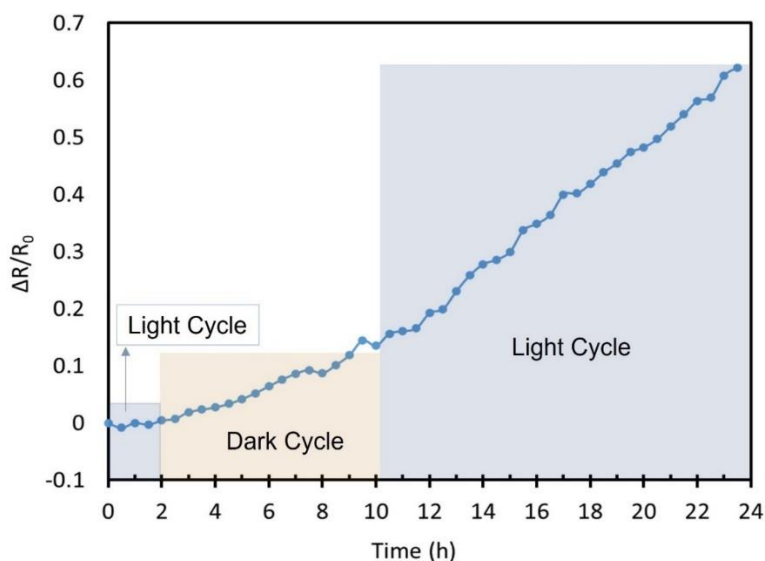
Figure 9*: Realtime Plant growth measurement. Image showing a stepwise growth of soybean over 24 hours,a rapid growth increase was observed during both light cycle and dark cycle. However the light cycle was more characterised with several short near stable growthwhile, total ΔR/R$_0$ amassed in 24 hours was 0.6, corresponding to approximately 373μm growth in one day.*

4.2 Discussion

In this study, we designed, developed an affordable PANI/elastic band strand strain sensor. We use the senor to measure plant growth (sunflower and soybean) in the stem. The morphological study shows the synergy between the elastic band substrate and PANI nanoparticles, PANI nanoparticle bonded to the substrate fiber making them conductive while the elastic band produce stretchability owing to their elastic properties (Figure 6).

The FTIR study conducted on our synthesized PANI (conductive polymer) shows various peaks indicating chemical bonds in our prepared clay (Figure 6). The peaks closely agree with PANI spectra reported in several previous study[49], hence our PANI was doped. Figure 7a is a curve showing the sensor response 100% stretch, the resistance of the sensor increases with increase in percentage strain. Figure 7d depict the sensor response

to 0.45mm 100 cycle tensile stretch, The sensor demonstrates good sensitivity and stability, the sensor responded to the repeated small stretch through increase in resistance and returned to the initial resistance after each strain unloading. The gauge factor of our strain sensor was 3.8 at 10% strain which is close to the gauge factor (3.9) for Au/PDMS strain sensor at 22% strain reported in previous study, reasonable to maintain stretchability and sensitivity, and fit enough to measure small stem increase per day [23] Our strain sensor demonstrated excellent electrical stability as the resistance remain stable for 5 days as depicted in Figure 7b, this suggests its fitness for longtime measurement and storage for future use. The resistance of the sensor increases due to temperature variation (Figure 7); however, our study was not negatively affected because the temperature range in our indoor growth chamber was from (20^0C to 25^0C) which fall under the sensor resistance stability range (20^0c to 30^0C). Realtime plant growth monitoring and measurement was carried out on internode below the apical meristem of sunflower and soybean. Previous studies measured plant growth rate by measuring fruit growth[20], [21], [52]. However, plant primary growth, i.e., elongation of the organs, happens near the tip of the shoot(stem) and root due to meristematic activity[22]. Meristems are stem cell responsible for plant increase in height and grith because of cell division [53]. Internodes are the stem between two nodes, growth happens in the apical meristem and the internodes, most especially the internode below the apical meristem in certain plants [22], [54], [55]. In Figure 8, day 1 curve shows a relationship between relative resistance ($\Delta R/R_0$) and plant growth, the $\Delta R/R_0$ increases with increasing plant stem (sensor length) over 24 hours. However, the plant growth has fluctuating pattern as major increase in relative resistance happens during the dark cycle and the light cycle was

mostly characterized by near stable $\Delta R/R_0$ and few short increases, this suggest that major rapid stem growth occur during the 8 hour dark cycle while the plant growth was nearly stable during the 16 hours light cycle. Day 2 growth curve follows the same profile as day 1, growth fluctuation was observed at almost the same time and interval as day 1 as the sunflower rapidly grow during the light cycle and the growth almost paused during the light cycle (Figure 8). The $\Delta R/R_0$ amassed by the PANI strain sensor corresponded to approximately 267 μm increase on day 1 and 355 μm increase on day 2 or an average of 311 μm per day. On the other hand, the experienced a rapid growth, during both dark cycle (8 hours) and light cycle (16 hours) as the $\Delta R/R_0$ rapidly increase for 24 hours (Figure 9). However, several slight near stable growth was observed in the light cycle period, suggesting that the plant growth slightly paused at several times and then the plant start growing again. The total $\Delta R/R_0$ amassed by our strain sensor in 24 hours for soybean was 0.6, corresponding to approximately 373μm growth per day. This type of fluctuating growth pattern in sunflower and soybean has been reported in previous studies [56], [57], Went reported this type of growth in tomatoes plant, in his study, he observed daily fluctuation in growth of tomatoes stem under 26^0C controlled temperature, the study identified maximum growth of the tomatoes stem in a day (70 to 90 percent) occur during darkness, whereas the slowest growth rate for each day was observed at daytime [55]. Our sensor recorded a rapid increase in stem growth during dark cycle and a near stable growth during the light cycle.

4.2.1 Limitation of the Strain Sensor

In this study, we developed and fabricated a strain sensor using a simple synthesis approach and a low cost elastic band substrate. We demonstrated the fitness of our sensor

to respond to strain and its applicability for measuring plant growth. However, few challenges in our method may impair the sensor performance.

Firstly, tensile stretch was applied on the sensor by manually slide the vernier jaw, this may give rise to potential error capable of affecting the sensor calibration accuracy.

Secondly, the resistance of the sensor was stable up to 300C, however, the resistance deflected at temperature above 300C. This limits the use of the sensor for outdoor application at higher temperature.

CHAPTER 5

CONCLUSION AND FUTURE WORK

5.1 Summary and Conclusion

In summary, we achieve the following through our approach:

1. An affordable strain sensor was fabricated simply by insitu dip coating PANI nanoparticles on a low-cost elastic band during chemical polymerization of aniline in HCl solution.

2. The morphology of the PANI coated elastic band shows a rough coated connected fiber strand, resulting in stable electrical properties.

3. The plant strain sensor detected a rhythmic growth in sunflower stem, exponential growth occurs during dark cycle while near stable growth occur during light cycle while the soybean majorly experienced an exponential growth during both light and dark cycle with several short time stable growth during the light cycle

4. For the period observed, the PANI-based strain sensor amassed an average of approximately 311 µm total stem elongation per day in sunflower, with major sprunt occurring for 8 hours dark cycle and approximately 373 µm total stem elongation in soybean.

Overall, our study demonstrated the applicability and sustainability of our low-cost strain sensor for measuring plant growth. The easy synthesis of PANI and the use of low-cost market available elastic band provides a new way of developing affordable plant strain sensor for deployment in precision agriculture.

5.2 Future Work

Plants are exposed to various environmental (abiotic) and biotic (bacteria, pathogen) stresses during growth stages[18], [58], [59] . Studies shows the relationship between plant volatile organic compounds (VOCs) emission and their metabolism[60]. Plants emit various VOCs as a defense or response to biotic and abiotic stressors[61]. Terpenes (Plant secondary metabolite), Green leaf volatiles, Methane, and Methyl Jasmonate has been identified as the VOCs emitted by plant, which not only plays signaling role in plant, but also involve in defense, communication, and pollination[60], [62]. Increase in plants VOCs emission when subjected to abiotic and Biotic stressors has been reported. Studies has shown that several terpenes like α-pinene, linalool, (E,E)-α-farnesen, and (D)-limonene was identified in the headspace of soybean plant under abiotic and biotic stresses[60], [63]–[67], this made VOCs profiling a new way for determining stresses in plants.

Recently, Chemiresistive sensor has been reported for their selective profiling of gases and volatile organic compounds in plants[16]. Chemiresistive sensors or chemistors measure resistance of a layer interacting with gas analytes. For example, a reduced graphene – based sensor was used to profile tomatoes volatile organic compounds VOCs upon exposure to pathogens and mechanical damage, the sensor classifies 13 different VOCs and early detects tomato late blight in the tomatoes plant [17]. We aim to use Mxene as sensing for detecting nutritional stresses in soybean, through profiling of terpenes emitted in its headspace. Mxene is a new two - dimensional transitional metal carbides with advantageous properties like large surface area, high Conductivity, porosity hydrophilicity and low density [68], [69].

REFERENCES

[1] UN FOOD AGENCY, "PLANTS, THE 'CORE BASIS FOR LIFE ON EARTH', UNDER INCREASING THREAT, WARNS UN FOOD AGENCY," *UN NEWS*, DEC. 02, 2019. HTTPS://NEWS.UN.ORG/EN/STORY/2019/12/1052591 (ACCESSED APR. 03, 2022).

[2] MSU EXTENSION, "ECOSYSTEM SERVICES," *NATIVE PLANTS AND ECOSYSTEM SERVICES*. HTTPS://WWW.CANR.MSU.EDU/NATIVEPLANTS/ECOSYSTEM_SERVICES (ACCESSED MAR. 04, 2022).

[3] E. PAPADOPOULOU AND K. CHRISSAFIS, "2 - PARTICLEBOARDS FROM AGRICULTURAL LIGNOCELLULOSICS AND BIODEGRADABLE POLYMERS PREPARED WITH RAW MATERIALS FROM NATURAL RESOURCES," IN *NATURAL FIBER-REINFORCED BIODEGRADABLE AND BIORESORBABLE POLYMER COMPOSITES*, A. K. LAU AND A. P.-Y. HUNG, EDS. WOODHEAD PUBLISHING, 2017, PP. 19–30. DOI: 10.1016/B978-0-08-100656-6.00002-9.

[4] D. JONES AND C. BRISCHKE, EDS., "2 - WOOD AS BIO-BASED BUILDING MATERIAL," IN *PERFORMANCE OF BIO-BASED BUILDING MATERIALS*, WOODHEAD PUBLISHING, 2017, PP. 21–96. DOI: 10.1016/B978-0-08-100982-6.00002-1.

[5] M. RAMESH, "9 - HEMP, JUTE, BANANA, KENAF, RAMIE, SISAL FIBERS," IN *HANDBOOK OF PROPERTIES OF TEXTILE AND TECHNICAL FIBRES*

(SECOND EDITION), A. R. BUNSELL, ED. WOODHEAD PUBLISHING, 2018, PP. 301–325. DOI: 10.1016/B978-0-08-101272-7.00009-2.

[6] A. SOFOWORA, E. OGUNBODEDE, AND A. ONAYADE, "THE ROLE AND PLACE OF MEDICINAL PLANTS IN THE STRATEGIES FOR DISEASE PREVENTION," *AFR J TRADIT COMPLEMENT ALTERN MED*, VOL. 10, NO. 5, PP. 210–229, AUG. 2013, ACCESSED: APR. 19, 2022. [ONLINE]. AVAILABLE: HTTPS://WWW.NCBI.NLM.NIH.GOV/PMC/ARTICLES/PMC3847409/

[7] S. HAZLEGREAVES, "THE ROLE OF PLANTS IN DRUGS AND MEDICINES," *OPEN ACCESS GOVERNMENT*, NOV. 23, 2020. HTTPS://WWW.OPENACCESSGOVERNMENT.ORG/THE-ROLE-OF-PLANTS-IN-DRUGS-AND-MEDICINES/98286/ (ACCESSED APR. 19, 2022).

[8] S. SAVARY, A. FICKE, J.-N. AUBERTOT, AND C. HOLLIER, "CROP LOSSES DUE TO DISEASES AND THEIR IMPLICATIONS FOR GLOBAL FOOD PRODUCTION LOSSES AND FOOD SECURITY," *FOOD SEC.*, VOL. 4, NO. 4, PP. 519–537, DEC. 2012, DOI: 10.1007/S12571-012-0200-5.

[9] O. US EPA, "THE SOURCES AND SOLUTIONS: AGRICULTURE," MAR. 12, 2013. HTTPS://WWW.EPA.GOV/NUTRIENTPOLLUTION/SOURCES-AND-SOLUTIONS-AGRICULTURE (ACCESSED JAN. 09, 2022).

[10] S. HUTSON, N. L. BARBER, J. F. KENNY, K. S. LINSEY, D. S. LUMIA, AND M. A. MAUPIN, "ESTIMATED USE OF WATER IN THE UNITED STATES IN 2000--USGS CIRCULAR 1268," *U.S. GEOLOGICAL SURVEY*, 2005. HTTPS://PUBS.USGS.GOV/CIRC/2004/CIRC1268/ (ACCESSED NOV. 17, 2021).

[11] M. MIN *ET AL.*, "DESIGN OF A HYPERSPECTRAL NITROGEN SENSING SYSTEM FOR ORANGE LEAVES," *COMPUTERS AND ELECTRONICS IN AGRICULTURE*, PP. 215–226, OCT. 2008, DOI: 10.1016/J.COMPAG.2008.03.004.

[12] PURDUERESEARCHPARK, *SENSOR GIVES FARMERS MORE ACCURATE READ ON PLANT HEALTH, PROVIDES VALUABLE CROP DATA*, (NOV. 01, 2018). ACCESSED: NOV. 17, 2021. [ONLINE VIDEO]. AVAILABLE: HTTPS://WWW.YOUTUBE.COM/WATCH?V=XXDCZCDAIEK

[13] T. W. SAPUTRA, R. E. MASITHOH, AND B. ACHMAD, "DEVELOPMENT OF PLANT GROWTH MONITORING SYSTEM USING IMAGE PROCESSING TECHNIQUES BASED ON MULTIPLE IMAGES," IN *PROCEEDING OF THE 1ST INTERNATIONAL CONFERENCE ON TROPICAL AGRICULTURE*, CHAM, 2017, PP. 647–653. DOI: 10.1007/978-3-319-60363-6_65.

[14] C. YANG, "HIGH RESOLUTION SATELLITE IMAGING SENSORS FOR PRECISION AGRICULTURE," *FRONT. AGR. SCI. ENG.*, VOL. 0, NO. 0, P. 0, 2018, DOI: 10.15302/J-FASE-2018226.

[15] M. ROY AND A. PRASAD, "RAMAN SPECTROSCOPY FOR NUTRITIONAL STRESS DETECTION IN PLANT VASCULAR TISSUE," *MATERIALIA*, P. 101474, 2022.

[16] H. IM, S. LEE, M. NAQI, C. LEE, AND S. KIM, "FLEXIBLE PI-BASED PLANT DROUGHT STRESS SENSOR FOR REAL-TIME MONITORING SYSTEM IN SMART FARM," *ELECTRONICS*, VOL. 7, NO. 7, ART. NO. 7, JUL. 2018, DOI: 10.3390/ELECTRONICS7070114.

[17] Z. LI *ET AL.*, "REAL-TIME MONITORING OF PLANT STRESSES VIA CHEMIRESISTIVE PROFILING OF LEAF VOLATILES BY A WEARABLE SENSOR," *MATTER*, VOL. 4, NO. 7, PP. 2553–2570, JUL. 2021, DOI: 10.1016/J.MATT.2021.06.009.

[18] Z. LI, J. ZHOU, T. DONG, Y. XU, AND Y. SHANG, "APPLICATION OF ELECTROCHEMICAL METHODS FOR THE DETECTION OF ABIOTIC STRESS BIOMARKERS IN PLANTS," *BIOSENSORS AND BIOELECTRONICS*, VOL. 182, P. 113105, JUN. 2021, DOI: 10.1016/J.BIOS.2021.113105.

[19] A. K. NASIR, M. TAJ, AND M. F. KHAN, "EVALUATION OF MICROSOFT KINECT SENSOR FOR PLANT HEALTH MONITORING," *IFAC-PAPERSONLINE*, VOL. 49, NO. 16, PP. 221–225, JAN. 2016, DOI: 10.1016/J.IFACOL.2016.10.041.

[20] W. TANG, T. YAN, J. PING, J. WU, AND Y. YING, "RAPID FABRICATION OF FLEXIBLE AND STRETCHABLE STRAIN SENSOR BY CHITOSAN-BASED WATER INK FOR PLANTS GROWTH MONITORING," *ADVANCED MATERIALS TECHNOLOGIES*, VOL. 2, NO. 7, P. 1700021, 2017, DOI: 10.1002/ADMT.201700021.

[21] W. TANG *ET AL.*, "RAPID FABRICATION OF WEARABLE CARBON NANOTUBE/GRAPHITE STRAIN SENSOR FOR REAL-TIME MONITORING OF PLANT GROWTH," *CARBON*, VOL. 147, PP. 295–302, JUN. 2019, DOI: 10.1016/J.CARBON.2019.03.002.

[22] L. M. SRIVASTAVA, *PLANT GROWTH AND DEVELOPMENT: HORMONES AND ENVIRONMENT*. ELSEVIER, 2002.

[23] J. NASSAR, S. KHAN, D. VILLALVA, M. NOUR, AND M. HUSSAIN, "COMPLIANT PLANT WEARABLES FOR LOCALIZED MICROCLIMATE AND PLANT GROWTH MONITORING," *NPJ FLEXIBLE ELECTRONICS*, VOL. 2, DEC. 2018, DOI: 10.1038/S41528-018-0039-8.

[24] E. SONG AND J.-W. CHOI, "CONDUCTING POLYANILINE NANOWIRE AND ITS APPLICATIONS IN CHEMIRESISTIVE SENSING," *NANOMATERIALS (BASEL)*, VOL. 3, NO. 3, PP. 498–523, AUG. 2013, DOI: 10.3390/NANO3030498.

[25] C. ZHANG, S. GOVINDARAJU, K. GIRIBABU, Y. S. HUH, AND K. YUN, "AGNWS-PANI NANOCOMPOSITE BASED ELECTROCHEMICAL SENSOR FOR DETECTION OF 4-NITROPHENOL," *SENSORS AND ACTUATORS B: CHEMICAL*, VOL. 252, PP. 616–623, 2017.

[26] I. Z. M. AHAD, S. W. HARUN, S. N. GAN, AND S. W. PHANG, "POLYANILINE (PANI) OPTICAL SENSOR IN CHLOROFORM DETECTION," *SENSORS AND ACTUATORS B: CHEMICAL*, VOL. 261, PP. 97–105, 2018.

[27] D. ZHANG, Z. WU, AND X. ZONG, "FLEXIBLE AND HIGHLY SENSITIVE H2S GAS SENSOR BASED ON IN-SITU POLYMERIZED SNO2/RGO/PANI TERNARY NANOCOMPOSITE WITH APPLICATION IN HALITOSIS DIAGNOSIS," *SENSORS AND ACTUATORS B: CHEMICAL*, VOL. 289, PP. 32–41, 2019.

[28] M. R. KARIM, M. M. ALAM, M. O. AIJAZ, A. M. ASIRI, F. S. ALMUBADDEL, AND M. M. RAHMAN, "THE FABRICATION OF A CHEMICAL SENSOR

WITH PANI-TIO 2 NANOCOMPOSITES," *RSC ADVANCES*, VOL. 10, NO. 21, PP. 12224–12233, 2020.

[29] X. X. GONG *ET AL.*, "FLEXIBLE STRAIN SENSOR WITH HIGH PERFORMANCE BASED ON PANI/PDMS FILMS," *ORGANIC ELECTRONICS*, VOL. 47, PP. 51–56, 2017.

[30] Y. FANG *ET AL.*, "SELF-HEALABLE AND RECYCLABLE POLYURETHANE-POLYANILINE HYDROGEL TOWARD FLEXIBLE STRAIN SENSOR," *COMPOSITES PART B: ENGINEERING*, VOL. 219, P. 108965, AUG. 2021, DOI: 10.1016/J.COMPOSITESB.2021.108965.

[31] F. JIN, D. LV, W. SHEN, W. SONG, AND R. TAN, "HIGH PERFORMANCE FLEXIBLE AND WEARABLE STRAIN SENSOR BASED ON RGO AND PANI MODIFIED LYCRA COTTON E-TEXTILE," *SENSORS AND ACTUATORS A: PHYSICAL*, VOL. 337, P. 113412, 2022.

[32] W. G. D. FERNANDO, "PLANTS: AN INTERNATIONAL SCIENTIFIC OPEN ACCESS JOURNAL TO PUBLISH ALL FACETS OF PLANTS, THEIR FUNCTIONS AND INTERACTIONS WITH THE ENVIRONMENT AND OTHER LIVING ORGANISMS," *PLANTS (BASEL)*, VOL. 1, NO. 1, PP. 1–5, FEB. 2012, DOI: 10.3390/PLANTS1010001.

[33] "STRESS_(PHYSICS)." HTTPS://WWW.CHEMEUROPE.COM/EN/ENCYCLOPEDIA/STRESS_%28PH YSICS%29.HTML (ACCESSED APR. 24, 2022).

[34] "12.3 STRESS, STRAIN, AND ELASTIC MODULUS - UNIVERSITY PHYSICS VOLUME 1 | OPENSTAX." HTTPS://OPENSTAX.ORG/BOOKS/UNIVERSITY-

PHYSICS-VOLUME-1/PAGES/12-3-STRESS-STRAIN-AND-ELASTIC-MODULUS (ACCESSED APR. 24, 2022).

[35] H. K. LICHTENTHALER, "THE STRESS CONCEPT IN PLANTS: AN INTRODUCTION," *ANN N Y ACAD SCI*, VOL. 851, PP. 187–198, JUN. 1998, DOI: 10.1111/J.1749-6632.1998.TB08993.X.

[36] T. GASPAR *ET AL.*, "CONCEPTS IN PLANT STRESS PHYSIOLOGY. APPLICATION TO PLANT TISSUE CULTURES," *PLANT GROWTH REGULATION*, VOL. 37, PP. 263–285, JAN. 2002, DOI: 10.1023/A:1020835304842.

[37] H. ZHANG, J. ZHU, AND Z. GONG, "ABIOTIC STRESS RESPONSES IN PLANTS | NATURE REVIEWS GENETICS." HTTPS://WWW.NATURE.COM/ARTICLES/S41576-021-00413-0 (ACCESSED APR. 24, 2022).

[38] A. GULL, A. A. LONE, AND N. U. I. WANI, *BIOTIC AND ABIOTIC STRESSES IN PLANTS*. INTECHOPEN, 2019. DOI: 10.5772/INTECHOPEN.85832.

[39] C. LI *ET AL.*, "MEASURING PLANT GROWTH CHARACTERISTICS USING SMARTPHONE BASED IMAGE ANALYSIS TECHNIQUE IN CONTROLLED ENVIRONMENT AGRICULTURE," *COMPUTERS AND ELECTRONICS IN AGRICULTURE*, VOL. 168, P. 105123, JAN. 2020, DOI: 10.1016/J.COMPAG.2019.105123.

[40] A. T. NACHAZEL, "WHAT IS A STRAIN GAUGE AND HOW DOES IT WORK?," *MICHIGAN SCIENTIFIC CORPORATION*, AUG. 13, 2020.

HTTPS://WWW.MICHSCI.COM/WHAT-IS-A-STRAIN-GAUGE/ (ACCESSED MAR. 24, 2022).

[41] T. AGARWAL, "TYPES OF STRAIN GAUGE : CHARACTERISTICS, ADVANTAGES & APPLICATIONS," *ELPROCUS - ELECTRONIC PROJECTS FOR ENGINEERING STUDENTS*, MAY 31, 2020. HTTPS://WWW.ELPROCUS.COM/TYPES-OF-STRAIN-GAUGE/ (ACCESSED JUL. 25, 2022).

[42] N. K AND C. SEKHAR ROUT, "CONDUCTING POLYMERS: A COMPREHENSIVE REVIEW ON RECENT ADVANCES IN SYNTHESIS, PROPERTIES AND APPLICATIONS," *RSC ADVANCES*, VOL. 11, NO. 10, PP. 5659–5697, 2021, DOI: 10.1039/D0RA07800J.

[43] "FLEXIBLE CONDUCTIVE POLYMER COMPOSITES IN STRAIN SENSORS[*]."
HTTPS://MANU56.MAGTECH.COM.CN/PROGCHEM/EN/10.7536/PC200322 (ACCESSED JUL. 25, 2022).

[44] ZH. A. BOEVA AND V. G. SERGEYEV, "POLYANILINE: SYNTHESIS, PROPERTIES, AND APPLICATION," *POLYM. SCI. SER. C*, VOL. 56, NO. 1, PP. 144–153, SEP. 2014, DOI: 10.1134/S1811238214010032.

[45] CHANNEGOWDA, *POLYANILINE : CONDUCTING POLYMER-SYNTHESIS, PROPERTIES AND APPLICATIONS*, (NOV. 25, 2020). ACCESSED: JUN. 10, 2022. [ONLINE VIDEO]. AVAILABLE: HTTPS://WWW.YOUTUBE.COM/WATCH?V=YGTBO5KDXEI

[46] N. Y. ABU-THABIT, "CHEMICAL OXIDATIVE POLYMERIZATION OF POLYANILINE: A PRACTICAL APPROACH FOR PREPARATION OF SMART CONDUCTIVE TEXTILES," *J. CHEM. EDUC.*, VOL. 93, NO. 9, PP. 1606–1611, SEP. 2016, DOI: 10.1021/ACS.JCHEMED.6B00060.

[47] Y. DU, K. CAI, AND S. SHEN, "FACILE PREPARATION AND CHARACTERIZATION OF GRAPHENE NANOSHEET/POLYANILINE NANOFIBER THERMOELECTRIC COMPOSITES," *FUNCTIONAL MATERIALS LETTERS*, VOL. 06, OCT. 2013, DOI: 10.1142/S179360471340002X.

[48] H. GUAN, L.-Z. FAN, H. ZHANG, AND X. QU, "POLYANILINE NANOFIBERS OBTAINED BY INTERFACIAL POLYMERIZATION FOR HIGH-RATE SUPERCAPACITORS," *ELECTROCHIMICA ACTA*, VOL. 56, NO. 2, PP. 964–968, 2010.

[49] H. K. CHAUDHARI AND D. S. KELKAR, "INVESTIGATION OF STRUCTURE AND ELECTRICAL CONDUCTIVITY IN DOPED POLYANILINE," *POLYMER INTERNATIONAL*, VOL. 42, NO. 4, PP. 380–384, 1997, DOI: 10.1002/(SICI)1097-0126(199704)42:4<380::AID-PI727>3.0.CO;2-F.

[50] B. QIU, Z. LI, X. WANG, L. XIAOYAN, AND J. ZHANG, "EXPLORATION ON THE MICROWAVE-ASSISTED SYNTHESIS AND FORMATION MECHANISM OF POLYANILINE NANOSTRUCTURES SYNTHESIZED IN DIFFERENT HYDROCHLORIC ACID CONCENTRATIONS," *JOURNAL OF POLYMER SCIENCE PART A: POLYMER CHEMISTRY*, VOL. 55, JUL. 2017, DOI: 10.1002/POLA.28707.

[51] A. R. REBELO, C. LIU, K.-H. SCHÄFER, M. SAUMER, G. YANG, AND Y. LIU, "POLY(4-VINYLANILINE)/POLYANILINE BILAYER-FUNCTIONALIZED BACTERIAL CELLULOSE FOR FLEXIBLE ELECTROCHEMICAL BIOSENSORS," *LANGMUIR*, VOL. 35, NO. 32, PP. 10354–10366, AUG. 2019, DOI: 10.1021/ACS.LANGMUIR.9B01425.

[52] H. H. HSU *ET AL.*, "SELF-POWERED AND PLANT-WEARABLE HYDROGEL AS LED POWER SUPPLY AND SENSOR FOR PROMOTING AND MONITORING PLANT GROWTH IN SMART FARMING," *CHEMICAL ENGINEERING JOURNAL*, VOL. 422, P. 129499, OCT. 2021, DOI: 10.1016/J.CEJ.2021.129499.

[53] K. LEHTILÄ AND A. SUNDS LARSSON, "MERISTEM ALLOCATION AS A MEANS OF ASSESSING REPRODUCTIVE ALLOCATION," IN *REPRODUCTIVE ALLOCATION IN PLANTS*, ELSEVIER, 2005, PP. 51–75. DOI: 10.1016/B978-012088386-8/50002-8.

[54] R. GROß-HARDT AND T. LAUX, "STEM CELL REGULATION IN THE SHOOT MERISTEM," *JOURNAL OF CELL SCIENCE*, VOL. 116, NO. 9, PP. 1659–1666, MAY 2003, DOI: 10.1242/JCS.00406.

[55] F. W. WENT, "PLANT GROWTH UNDER CONTROLLED CONDITIONS. II. THERMOPERIODICITY IN GROWTH AND FRUITING OF THE TOMATO," *AMERICAN JOURNAL OF BOTANY*, VOL. 31, NO. 3, PP. 135–150, 1944, DOI: 10.2307/2437636.

[56] S. PERILLI, R. DI MAMBRO, AND S. SABATINI, "GROWTH AND DEVELOPMENT OF THE ROOT APICAL MERISTEM," *CURRENT OPINION*

IN PLANT BIOLOGY, VOL. 15, NO. 1, PP. 17–23, FEB. 2012, DOI: 10.1016/J.PBI.2011.10.006.

[57] A. DOBRESCU, L. C. T. SCORZA, S. A. TSAFTARIS, AND A. J. MCCORMICK, "A 'DO-IT-YOURSELF' PHENOTYPING SYSTEM: MEASURING GROWTH AND MORPHOLOGY THROUGHOUT THE DIEL CYCLE IN ROSETTE SHAPED PLANTS," *PLANT METHODS*, VOL. 13, P. 95, NOV. 2017, DOI: 10.1186/S13007-017-0247-6.

[58] Y.-S. KU, M. SINTAHA, M.-Y. CHEUNG, AND H.-M. LAM, "PLANT HORMONE SIGNALING CROSSTALKS BETWEEN BIOTIC AND ABIOTIC STRESS RESPONSES," *INT J MOL SCI*, VOL. 19, NO. 10, P. E3206, OCT. 2018, DOI: 10.3390/IJMS19103206.

[59] W. ZHANG, F. ZHAO, L. JIANG, C. CHEN, L. WU, AND Z. LIU, "DIFFERENT PATHOGEN DEFENSE STRATEGIES IN ARABIDOPSIS: MORE THAN PATHOGEN RECOGNITION," *CELLS*, VOL. 7, NO. 12, P. 252, DEC. 2018, DOI: 10.3390/CELLS7120252.

[60] L. COPOLOVICI, A. C. POPITANU, AND D.-M. COPOLOVICI, "VOLATILE ORGANIC COMPOUND EMISSION AND RESIDUAL SUBSTANCES FROM PLANTS IN LIGHT OF THE GLOBALLY INCREASING CO2 LEVEL," *CURRENT OPINION IN ENVIRONMENTAL SCIENCE & HEALTH*, VOL. 19, P. 100216, FEB. 2021, DOI: 10.1016/J.COESH.2020.10.004.

[61] W. WANG, B. VINOCUR, AND A. ALTMAN, "PLANT RESPONSES TO DROUGHT, SALINITY AND EXTREME TEMPERATURES: TOWARDS

GENETIC ENGINEERING FOR STRESS TOLERANCE," *PLANTA*, VOL. 218, NO. 1, PP. 1–14, NOV. 2003, DOI: 10.1007/S00425-003-1105-5.

[62] D. K. FARMER AND M. RICHES, "MEASURING BIOSPHERE-ATMOSPHERE EXCHANGE OF SHORT-LIVED CLIMATE FORCERS AND THEIR PRECURSORS," *ACC CHEM RES*, VOL. 53, NO. 8, PP. 1427–1435, AUG. 2020, DOI: 10.1021/ACS.ACCOUNTS.0C00203.

[63] R. DEL ROSARIO, B. O. DE LUMEN, T. HABU, R. A. FLATH, T. R. MON, AND R. TERANISHI, "COMPARISON OF HEADSPACE OF VOLATILES FROM WINGED BEANS AND SOYBEANS," *J. AGRIC. FOOD CHEM.*, VOL. 32, NO. 5, PP. 1011–1015, SEP. 1984, DOI: 10.1021/JF00125A015.

[64] J. LIU *ET AL.*, "GENOME-WIDE ANALYSIS OF TERPENE SYNTHASES IN SOYBEAN: FUNCTIONAL CHARACTERIZATION OF GMTPS3," *GENE*, VOL. 544, NO. 1, PP. 83–92, JUL. 2014, DOI: 10.1016/J.GENE.2014.04.046.

[65] M. F. F. MICHEREFF *ET AL.*, "VOLATILES MEDIATING A PLANT-HERBIVORE-NATURAL ENEMY INTERACTION IN RESISTANT AND SUSCEPTIBLE SOYBEAN CULTIVARS," *J CHEM ECOL*, VOL. 37, NO. 3, PP. 273–285, MAR. 2011, DOI: 10.1007/S10886-011-9917-4.

[66] T. R. WINTER AND M. ROSTÁS, "NITROGEN DEFICIENCY AFFECTS BOTTOM-UP CASCADE WITHOUT DISRUPTING INDIRECT PLANT DEFENSE," *J CHEM ECOL*, VOL. 36, NO. 6, PP. 642–651, JUN. 2010, DOI: 10.1007/S10886-010-9797-Z.

[67] J. ZHU AND K.-C. PARK, "METHYL SALICYLATE, A SOYBEAN APHID-INDUCED PLANT VOLATILE ATTRACTIVE TO THE PREDATOR

COCCINELLA SEPTEMPUNCTATA," *J CHEM ECOL*, VOL. 31, NO. 8, PP. 1733–1746, AUG. 2005, DOI: 10.1007/S10886-005-5923-8.

[68] M. ALHABEB *ET AL.*, "GUIDELINES FOR SYNTHESIS AND PROCESSING OF TWO-DIMENSIONAL TITANIUM CARBIDE (TI3C2TX MXENE)," *CHEM. MATER.*, VOL. 29, NO. 18, PP. 7633–7644, SEP. 2017, DOI: 10.1021/ACS.CHEMMATER.7B02847.

[69] K. MALESKI, V. N. MOCHALIN, AND Y. GOGOTSI, "DISPERSIONS OF TWO-DIMENSIONAL TITANIUM CARBIDE MXENE IN ORGANIC SOLVENTS," *CHEM. MATER.*, VOL. 29, NO. 4, PP. 1632–1640, FEB. 2017, DOI: 10.1021/ACS.CHEMMATER.6B04830.